

# Post-Cracking Behaviour of High Strength Fiber Concrete Prediction and Validation

Andrejs Krasnikovs, Olga Kononova, Amjad Khabbaz, Edgar Machanovsky and Artur Machanovsky

**Abstract**—Fracture process in mechanically loaded steel fiber reinforced high-strength (SFRHSC) concrete is characterized by fibers bridging the crack providing resistance to its opening. Structural SFRHSC fracture model was created; material fracture process was modeled, based on single fiber pull-out laws, which were determined experimentally (for straight fibers, fibers with end hooks (Dramix), and corrugated fibers (Tabix)) as well as obtained numerically (using FEM simulations). For this purpose experimental program was realized and pull-out force versus pull-out fiber length was obtained (for fibers embedded into concrete at different depth and under different angle). Model predictions were validated by 15x15x60cm prisms 4 point bending tests. Fracture surfaces analysis was realized for broken prisms with the goal to improve elaborated model assumptions. Optimal SFRHSC structures were recognized.

**Keywords**—crack, fiber concrete, fiber pull-out, strength.

## I. INTRODUCTION

THE concrete compressive strength increase is leading to more brittle such material mechanical behavior. One of the ways how to increase the safety of material in loaded structures is to add short steel fibers. Fibers are possible to use in combination with some kind of continuous reinforcement (steel or composite rebars, etc.), as well as to replace continuous reinforcement by fibers. At the same time, a high content of steel fibers negatively affects the mix workability. Therefore for the aim of good workability of the mix, steel fibers are limited both by their maximal content, geometry (chemical bond between steel fiber and concrete matrix is weak and fibers are anchoring in the matrix mainly geometrically and by frictional forces) and length. Increasing applied loads the matrix fracture process is initialized, micro cracks start to open to grow and to coalescent finally forming one or few macro cracks. Steel fibers are bridging the crack.

## II. SINGLE FIBER PULL-OUT EXPERIMENTAL INVESTIGATION

### Single fiber pull-out law experimental investigations for

Andrejs Krasnikovs is with the Concrete Mechanics lab. and Institute of Mechanics, Riga Technical University, Riga, Latvia, (e-mail:akrasn@latnet.lv).

Olga Kononova is with the Institute of Mechanics, Riga Technical University, Riga, Latvia, (e-mail:olga.kononova@gmail.com).

Amjad Khabbaz is with the Concrete Mechanics lab, Riga Technical University, Riga, Latvia (amjad.khabbaz@rtu.lv).

Edgar Machanovsky is with the Institute of Mechanics, Riga Technical University, Riga, Latvia, (e-mail:gavrikl@inbox.lv).

Artur Machanovsky is with the Institute of Mechanics, Riga Technical University, Riga, Latvia, (e-mail:arturmacanovskis@inbox.lv).

some steel fibers pulled out of the conventional concrete were reported in [1, 2]. Follows types of 50 mm long steel fibers were used in our investigation – straight fibers, fibers with end hooks (Dramix), and corrugated form fibers (Tabix) [3, 4].

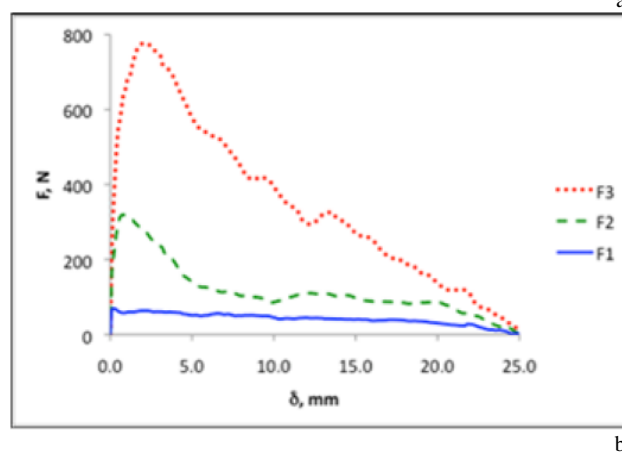
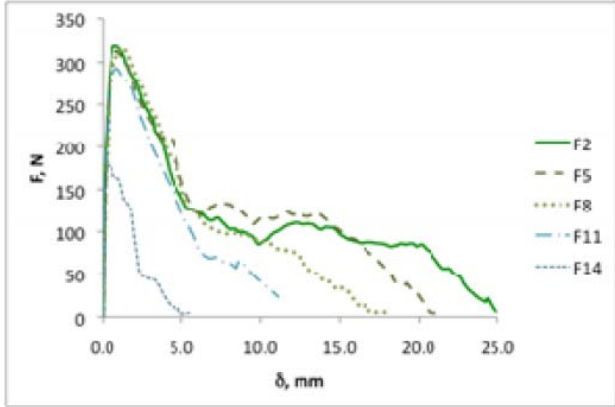


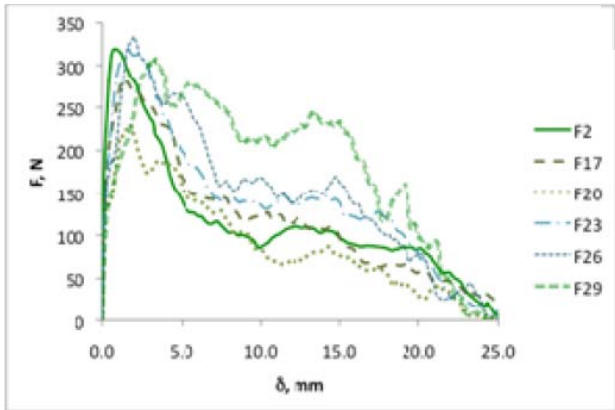
Fig. 1 a) the pull-out specimen's mould; b) pull-out curves ( $L = 25$  mm,  $\alpha = 0^\circ$ ) for: F1 – straight (lower curve); F2 – hooked-end (middle curve); F3 – corrugated (upper curve).

The pull-out test samples were manufactured in plywood moulds with configuration given in Fig.1.a. A thin plastic film was used also as a separator between the two halves of the specimen as shown in Fig.1.a. All pull-out specimens were tested in tensile testing machine Zwick/Roell Z150 (grips with 1kN dynamometer were used), combined with video extensometer "Messphysik" (for displacement measuring). Experiments were realized for fiber embedment lengths  $L=5$ mm; 10mm; 15mm; 20mm; 25mm and orientation angles  $\alpha= 0^\circ; 10^\circ; 20^\circ; 30^\circ; 45^\circ; 60^\circ$  (the results patterns are

shown in Fig.1.b and Fig.2, 3. Because of an experimental data scatter nine specimens were tested with the same geometry and concrete matrix properties (three different compressive strength matrixes were investigated) after that average values and data dispersions were obtained.

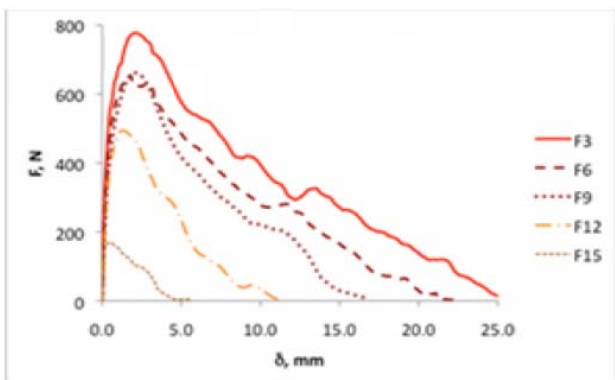


a)

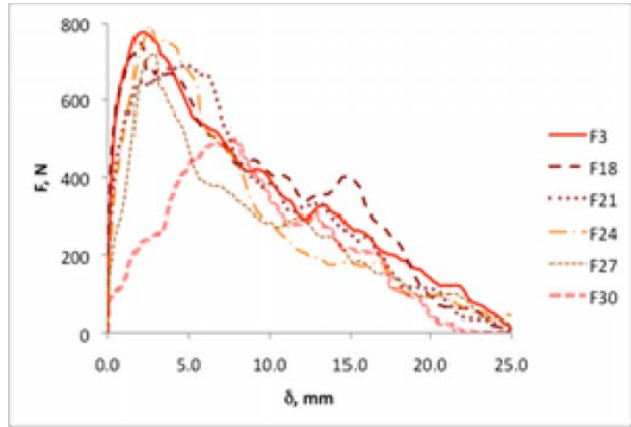


b)

Fig. 2 The pull-out curves for hooked-end fibers: a) under the angle  $\alpha = 0^\circ$  and embedded at different depth: F2 -  $L = 25$  mm; F5 -  $L = 20$  mm; F8 -  $L = 15$  mm; F11 -  $L = 10$  mm; F14 -  $L = 5$  mm; b) embedded at the depth  $L = 25$  mm, under the different angle: F2 -  $\alpha = 0^\circ$ ; F17 -  $\alpha = 10^\circ$ ; F20 -  $\alpha = 20^\circ$ ; F23 -  $\alpha = 30^\circ$ ; F26 -  $\alpha = 45^\circ$ ; F29 -  $\alpha = 60^\circ$



a)

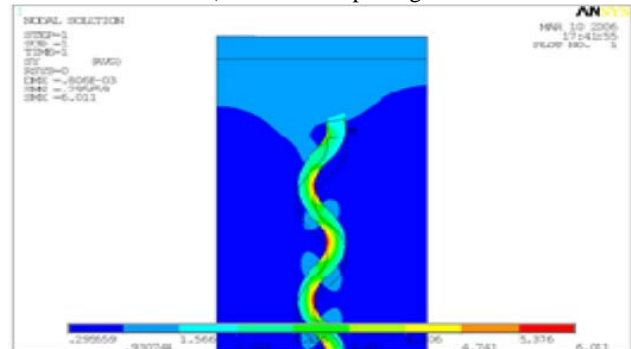


b)

Fig. 3 a) The pull-out curves for corrugated fibers: a) under the angle  $\alpha = 0^\circ$  and embedded at different depth: F3 -  $L = 25$  mm; F6 -  $L = 20$  mm; F9 -  $L = 15$  mm; F12 -  $L = 10$  mm; F15 -  $L = 5$  mm; b) embedded at the depth  $L = 25$  mm, under the different angle: F3 -  $\alpha = 0^\circ$ ; F18 -  $\alpha = 10^\circ$ ; F21 -  $\alpha = 20^\circ$ ; F24 -  $\alpha = 30^\circ$ ; F27 -  $\alpha = 45^\circ$ ; F30 -  $\alpha = 60^\circ$

### III. MICROMECHANICAL MODELING

Pulled out fibers are providing resistances to crack propagation and crack opening. Additionally, at initial stage of crack opening rough aggregates in concrete are bridging the crack tip. Steel fibers producers are representing on the market variety of different geometry products. Using each fiber type in combination with corresponding properties concrete matrix is possible to obtain fiberconcrete stable (not rapidly decreasing) post cracking mechanical behavior. Important is to perform a detailed micro-mechanical investigation of fiber pull-out process in order to understand and to characterize the crack propagation mechanics in SFHPRC structural elements. Can be recognized four main stages of single fibre pull-out process [5]: a) fibre and concrete matrix are bonded together (perfect bond), all deformations in system are elastic; b) cylindrical delamination crack is starting from the outer concrete block surface to propagate into material between fibre and concrete matrix [5-7]. Crack is growing at the beginning by modes one and two and with an increase of the debond depth mainly by mode 2 (with friction); c) when fibre embedment is small (short fibre or pulling out



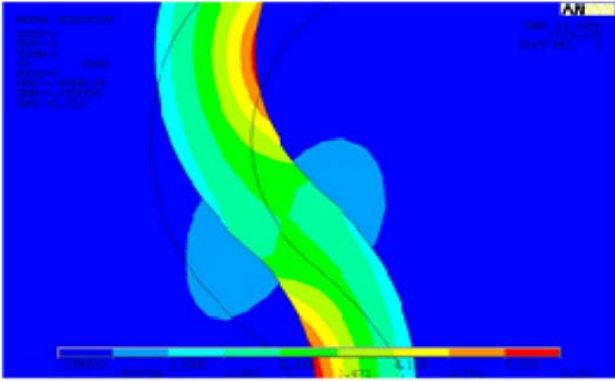


Fig. 4 A tensile stress  $\sigma_{yy}$  in concrete and steel corrugated fibre subjected to external pulling load in the case of perfect bond between them (all fiber embedded length (left picture), fiber single wave (right picture)).

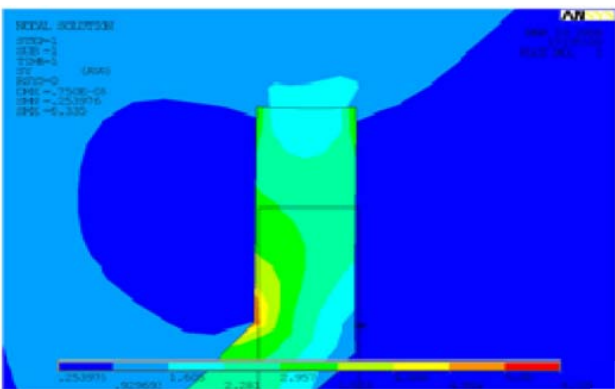
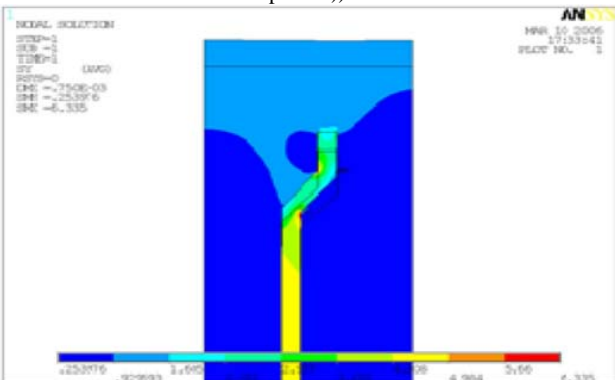


Fig. 5 A tensile stress  $\sigma_{yy}$  in concrete and steel hooked-end fibre subjected to external pulling load in the case of perfect bond between them (all fiber embedded length (left picture), fiber hooked end (right picture))

the shorter end of the fibre which is bridging the crack) delamination is reaching all embedded length of the fibre after that fibre with friction is pulling out. If fibre embedment is large, fibre is breaking at the length  $L$  in concrete, after what free fibre end with friction is pulling out of matrix [5]; d) stretched fibre breaks out of concrete. Fibers breaking in material according scenario a-c are responsible to fiberconcrete post-cracking quasi-plastic behaviour. Simulations have been done by ANSYS software. Three

numerical 2D and 3D models were investigated: 1) single steel fibre is embedded into concrete matrix with perfect bond between them and subjected to external pulling load (samples of calculated stress fields in concrete and fibre around corrugated and hooked-end fibers are shown in Fig.4 and Fig.5); 2) the situation, when between pulling out fiber and matrix is growing delamination. In delaminated area fiber and matrix are debonded. Each mutual motion in this zone performs with friction. Numerically this situation was simulated

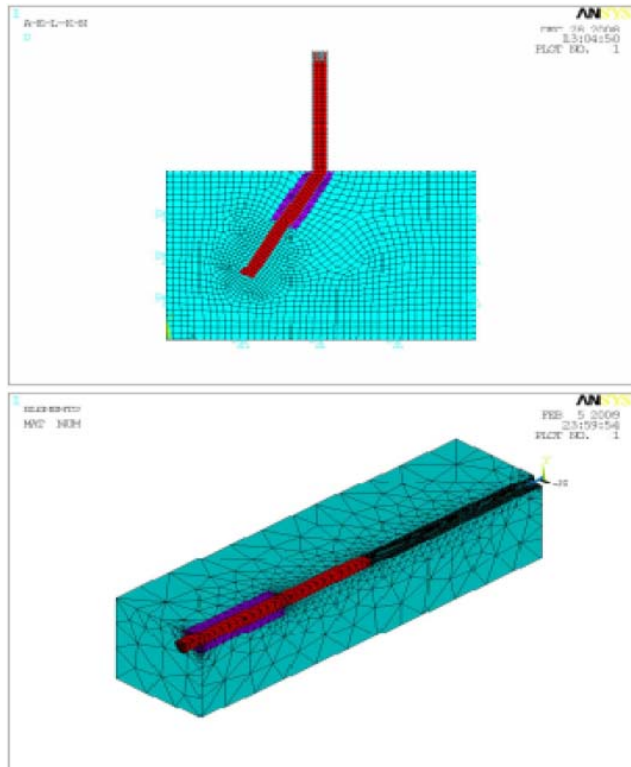
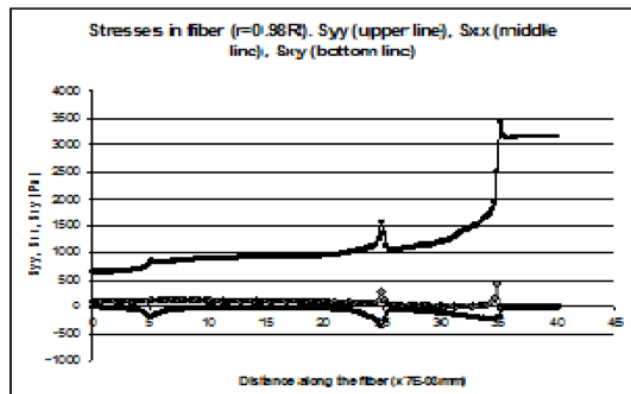


Fig. 6 The numerical model for fiber partially debonded in concrete matrix (2D model for the fiber is pulling out of concrete under the angle  $\alpha = 30^\circ$  (left picture); 3D model for the fiber is pulling out of concrete under the angle  $\alpha = 0^\circ$  (right picture)).



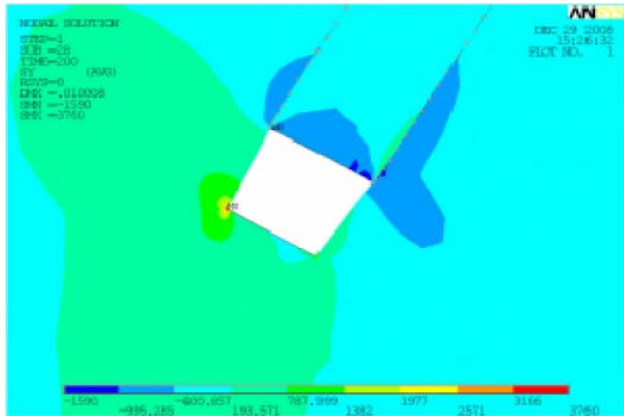


Fig. 7 2D stresses in fiber ( $r=0.98R$ ),  $\sigma_{yy}$ - upper line,  $\sigma_{xx}$ - middle line,  $\sigma_{xy}$ - bottom line ) fiber is pulling out of concrete under the angle  $\alpha = 0^\circ$  (left picture) and 2D stresses in fiber and matrix during debonded fiber is sliding out of concrete with friction (contact FE were used for modeling) under the angle  $\alpha = 30^\circ$  (right picture)

incorporating soft interlayer between fiber and matrix (in Fig.6 left picture is corresponding to 2D model, right picture is corresponding to 3D model). Stresses in the fiber along the line parallel to fiber axis in vicinity to interface with matrix (0.98 of fiber radius) are shown in Fig.7 (left picture). Peaks on the lines (going from left to right) corresponds to: a) fiber end in concrete (small peaks); b) beginning of delamination zone (middle peaks); c) outer surface of concrete block (right peaks). Stress peaks at the front of delamination zone (corresponds to singularities in classical solution) are explaining mechanism of fiber break at some distance in concrete volume, because during delamination growth elevated overstress is crossing different fiber crossections in concrete till the weakest is reached. Simultaneously overstress is decreasing going deeper along the debonded fiber –concrete matrix interface (starting from the outer surface of concrete block) and increasing with fiber/matrix interface friction increase (corresponds to concrete matrix with higher compressive strength). At the same moment overloads in the matrix are rising into concrete body micro-cracks formation around the fiber. These cracks were observed experimentally. Simplified models for stress distribution around pulling out fiber were discussed in [7]; 3) numerical model were elaborated to describe fiber end sliding motion after the break in the concrete matrix or in the case when delamination reach the embedded end of fiber. FEM model with FE contact elements between fiber and matrix were exploited (see Fig.7 right picture). Numerically calculated force – pulled out fiber length were compared with experimentally measured and friction coefficient values between fiber and concrete matrix during fiber sliding out of matrix were obtained.

#### IV. MACROMECHANICAL MODELING

The construction member cracking and post cracking behavior was investigated experimentally testing notched SFHPC prisms (15x15x60cm) under 4-point bending (till

macro-crack mouth opening displacement (CMOD) reaches 6-10mm) and obtaining applied load – CMOD diagrams. The same process was simulated numerically on the base of elaborated structural macro-crack (bridged by fibers) opening model. Elaborated model takes into account the types of fibers were used and also the quantity of each fiber type in the concrete mix. It had been shown by many research papers [see references in 2-5] that the amount and type of fibers used in FRC mix significantly influence the load bearing capacity and behavior of the FRC structural element. A SFRC beam with chaotic fiber orientation

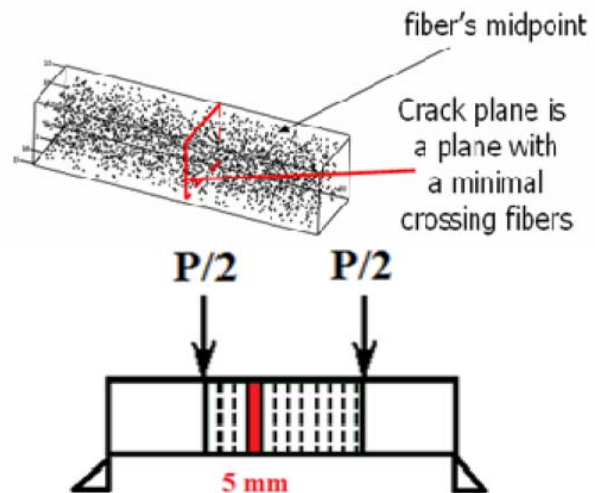


Fig. 8 Fibers midpoint coordinates generated by single run of Monte-Carlo simulation. In every simulation fibers midpoint coordinates and spatial orientation angles were obtained (left picture). Crack's plane was obtained as a plane with a minimal number of fibers crossing it (right picture)

subjected to four point bending was modeled. A random distribution function was applied to determine location and orientation angle of each fiber. Monte-Carlo simulations were performed to obtain each fiber location and orientation in every particular SFRHPC prism (Fig.8 left picture). After that, weakest (critical) crossection was recognized as the crossection with the smallest amount of fibers crossing it. In the critical cross-section the number, location and spatial orientation of each fiber was known. It's meant that orientation angle and embedded length of every fiber crossing the cross-section is known with respect to the plane of cross-section (Fig.8 right picture). The crack starts to open (this procedure in the model is happened step by step increasing crack mouth opening displacement (CMOD)). At every step (known value of  $CMOD=\delta$  (see Fig.9)) every fiber crossing the crack starts to pull out. Information about every particular fiber location orientation, type and embedment length is known previously from the simulation procedure and is keeping in the model. Then the corresponding data from the database file which contains all information from pull-out experiments with single fibers must be correctly read and applied (see Fig.9). Load is

bearing by every particular fiber is crossing the crack, denotes depending on the fiber location,

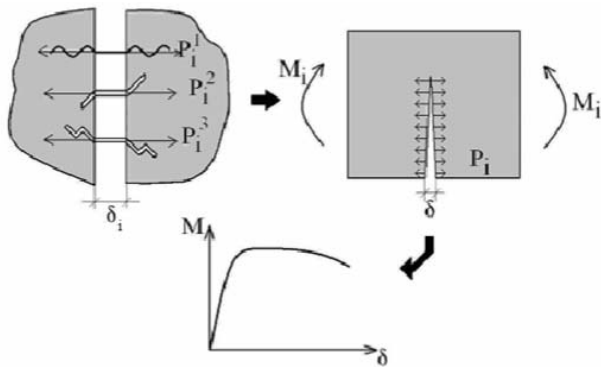
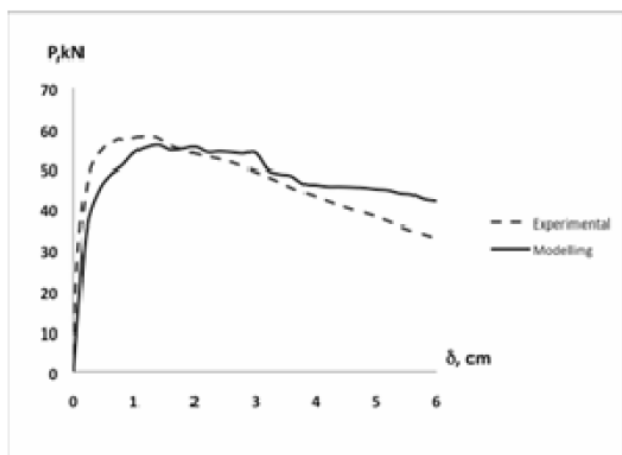


Fig. 9 Model description

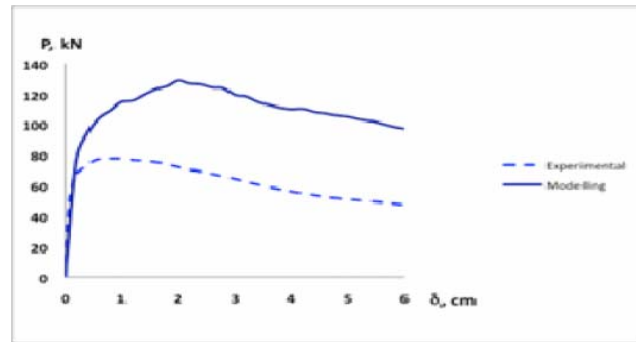
orientation (to crack plane) and its location point opening  $\delta_i$  (see Fig.9). Summarizing all local loads we are obtaining bending moment working in the crack plane and corresponding value of external force. Performing numerical simulation of above mentioned crack opening process we are obtaining theoretical applied load- CMOD curve.

#### V. MODEL VERIFICATION

The proposed model was applied for SFRC and SFRHPC behaviour prediction with various fibre types and concentrations. SFRC mixes with fibre concentration within the range from  $50 \text{ kg/m}^3$  to  $450 \text{ kg/m}^3$  and still high workability were studied. In Fig. 10 is shown model prediction comparison with experiment for SFRHPC having fibre cocktails  $150 \text{ kg/m}^3$  and  $280 \text{ kg/m}^3$ . Increasing the fiber amount in concrete is increasing the difference between prediction and experimental data. Explanation of this phenomenon may be fibers non-homogeneous distribution in the prism volume, as well as formation of internal surfaces (obtained during filling the mould) with oriented fibers (fibers orientation can't be supposed as purely chaotic).



a)



b)

Fig. 10 Model predicted load- CMOD (mm) dependence (-) in comparison with experiment (...) for SFRHPC containing: a)  $150 \text{ kg/m}^3$ ; b)  $280 \text{ kg/m}^3$  different type steel fibers. Beams sizes were  $15 \times 15 \times 60 \text{ cm}$ .

#### VI. CONCLUSION

Detailed structural SFRHPC post-cracking behavior model was elaborated and numerically analyzed. The validity of the proposed model has been proved for SFRC and SFRHPC beams with fiber concentrations up to  $450 \text{ kg/m}^3$ . Prediction results comparison with experiments was allowed to appreciate such factors as: fibers distribution, orientation, and way of anchoring as well as matrix strength influence on non-linear post-cracking SFRC mechanical behavior.

#### ACKNOWLEDGMENT

This work has been supported by the European Social Fund within the Project Nr. 2009/0201/1DP/1.1.1.2.0/09/APIA/VIAA/112 "Nanotechnological research of the mechanical element surface and internal structure in mechanical engineering".

#### REFERENCES

- [1] Armelin HS, Bantia N 'Predicting the flexural post cracking performance of steel fiber reinforced concrete from the pullout of single fibers', *ACI Mater J* 94:18–31.
- [2] Robins P, Austin S, Jones P 'Pull-out behavior of hooked steel fibers', *Mater Struct* 35:434–442.
- [3] Krasnikovs A. & Kononova O., 'Strength Prediction for Concrete Reinforced by Different Length and Shape Short Steel Fibers', *Sc. Proceedings of Riga Technical University. Transport and Engineering*, 6, vol.31, 2009, pp.89-93.
- [4] Krasnikovs A., Kononova O. & Pupurs A., 'Steel Fiber Reinforced Concrete Strength' *Sc. Proceedings of Riga Technical University. Transport and Engineering*, 6, vol.28, Riga, 2008, pp. 142-150.
- [5] A. Krasnikovs, A. Khabbaz, I. Telnova, A. Machanovsky and J. Klavinsh 'Numerical 3D investigation of non-metallic (glass, carbon) fiber pull-out micromechanics (in concrete matrix)', *Sc. Proceedings of Riga Technical University, Transport and engineering*, 6, vol. 33, 2010, p.103-108.
- [6] Pupurs A., Krasnikovs A. and Varna J. 'Energy release rate based fiber/matrix debond growth in fatigue'. Part II: Debond growth analysis using Paris law. *Mechanics of Advanced Materials and Structures*, Submitted 2009.
- [7] Victor C. Li., 'On Engineered Cementitious Composites a Revue of the Material an it's Applications', *J. of Advanced Concrete Technology*, Vol.1, No3, 2003, pp. 215-230.